Contemporary spatio-temporal patterns of snow cover over the Drakensberg

N. Mulder and S.W. Grab*

Sixteen years of low-resolution Landsat 5 and 7 satellite images were used to construct Boolean images of snow cover over the Drakensberg through a GIS. Contemporary patterns of snow cover, including altitudinal variations, were determined for individual months and various seasons. The seasonal occurrence and spatial influence of various snow-producing weather systems were determined through remote sensing and the consultation of daily climate data and synoptic charts. A proportional relationship was found between altitude of snow-covered pixels and the number of occurrences that pixels were covered in snow. The highest incidence and most widespread snow cover occurred from June to August; spring snow occurred preferentially in the central and southern Drakensberg regions. Cold fronts and associated cut-off lows accounted for about 80% of snow cover over the Drakensberg.

Key words: Drakensberg, satellite images, snow-cover patterns, weather systems

Introduction

Given limited meteorological records, little is known about the spatial and temporal patterns of snow cover over the Drakensberg. Although it is commonly assumed that snowfalls in the region occur approximately eight times per annum,[1–3] information on monthly or seasonal snowfall trends and the longevity of snow patches is absent. A previous study[4] used high-resolution thematic mapper (TM) images to assess site-specific variables (latitude, topographic orientation, distance from the escarpment) influencing snow cover. We used 16 years of low-resolution composite satellite images to determine macro-scale spatial and temporal patterns of snow cover over the Drakensberg. The new information should be of interest to ecologists, geomorphologists, climatologists, tourism developers and managers concerned with the Drakensberg and eastern Lesotho Highlands.

Browse images were acquired from Landsat 5 and 7 satellites using TM and enhanced thematic mapper (ETM)+ sensors respectively; these have a 360 m pixel resolution, which was the highest resolution obtainable within our budget at the time of analysis. Although accurate snow mapping in association with local topography is therefore not possible, it does permit multiple macro-scale assessments of snow cover distribution. The advantage of using low-resolution images is the availability of numerous historical images dating back to 1989. A total of 41 low-resolution images (Path 169; Row 80) with observable snow present, and with insignificant or no cloud cover, were identified for the period from 1989 to 2004 (Table 1). Emphasis is placed on the temporal component of these low-resolution images, as a relatively high number of images from multiple years are necessary to determine seasonal trends in snow cover. These data are also used to examine snow occurrence and distribution associated with various snow-producing climatic events during different months or seasons. Cross-checking of remotely sensed data with climatic data indicates that not all snow events are evident in the satellite imagery due to temporal staging of satellite overpasses. Occasional snowfall events have been recorded in weather reports, yet fail to feature on satellite images as the data were presumably only captured after the snow had ablated. It should also be noted that snowfall events producing thin and small-scale snow cover may not be visible at a 360 m resolution. Hence, this study particularly focused on snowfalls that produced substantial (although sometimes localised) snow cover, and which consequently may have impacted human livelihoods, livestock grazing and ecosystem functioning.

Table 1. Snow-covered area (km^2) derived from predominantly low-resolution images.

No.	Date of image	Landsat platform	Snow-covered area (km^2)	Comments
1	31 Jul 1989	5	45.32	
2	16 Aug 1989	5	32.48	
3	3 Aug 1990	5	155.10	
4	19 Aug 1990	5	50.88	
5	4 Sep 1990	5	41.86	
6	22 Oct 1990	5	477.90	
7	19 Jun 1991	5	409.73	
8	8 Aug 1992	5	242.78	
9	8 Jun 1993	5	7.90	
10	24 Apr 1994	5	97.56	
11	29 Jul 1994	5	1908.76	
12	30 Aug 1994	5	24.94	
13	30 Jun 1995	5	75.70	
14	18 Sep 1995	5	21.49	
15	20 Oct 1995	5	99.16	
16	31 May 1996	5	9.26	
17	18 Jul 1996	5	2124.74	
18	19 Aug 1996	5	1478.16	
19	20 Sep 1996	5	81.63	
20	6 Oct 1996	5	161.28	
21	5 May 1997	5	666.34	
22	21 Jul 1997	5	946.05	
23	22 Aug 1997	5	408.50	
24	25 Aug 1998	5	1713.77	
25	12 Aug 1999	5	9.76	
26	10 May 2000	7	205.24	Sensor saturation (cloud)
27	30 Jun 2001	7	1990.14	
28	9 Aug 2001	7	6.79	
29	10 Sep 2001	7	14.08	Sensor saturation (cloud)
30	8 May 2002	7	476.91	
31	24 May 2002	7	802.43	
32	9 Jun 2002	7	367.63	
33	25 Jun 2002	7	1200.06	
34	11 Jul 2002	7	357.75	
35	27 Jul 2002	7	1663.64	
36	12 Aug 2002	7	448.88	
37	13 Sep 2002	7	24.32	
38	22 Jun 2004	7	7.16	
39	8 Jul 2004	7	302.79	
40	9 Aug 2004	7	17.17	
41	10 Sep 2004	7	744.64	Sensor saturation (cloud)

Methods

Our earlier remote sensing study[4] explored some of the literature which describes the most suitable methods for mapping snow. We applied some of the suggested standard methods to our

School of Geography, Archaeology and Environmental Studies, University of the Witwatersrand, Private Bag 3, WITS 2050, South Africa.

*Author for correspondence E-mail: stefan.grab@wits.ac.za

previous study and found these to be most useful, and thus proposed a similar approach for this study. Forty-one images were imported into a geographic information system (GIS) and georegistered against a digital elevation model (DEM), which was used as a base map to ensure an accurate overlay. DEMs allow remotely-sensed data to be seen in a quantitative altitudinal component through the use of GIS, and are thus favoured for snow mapping.[5] Initially, the pre-processed images used as primary data did not accurately meet the given geo-references. On occasions, two separate images had to be merged to cover the full study region (from 28°37′S to 29°55′S and 28°45′E to 29°30′ E) (Fig. 1). Twenty test locations were used to confirm the georegistration. Ultimately, random sampling confirmed that an error of less than 1 pixel (360 m) was obtained across all 41 images.

As the images were already in colour composite form, a fine unsupervised classification of the images was performed using Idrisi 2.0, which enabled the identification of snow cover once areas below 2 600 m above sea level (a.s.l.) had been masked out. Clustering was performed separately on each image (i.e. one image per date). By masking out areas below 2 600 m a.s.l., the accuracy of classification was substantially increased, with individual images confirmed through visual analysis. The fine unsupervised classification is a specific Idrisi algorithm and option, in which the dominant spectral response patterns that occur within an image are extracted. The broad and fine generalisation levels use different decision rules to determine the number of clusters or classes. The broad classification groups modes into different classes, separated at their 'valleys', whilst the fine classification manages to divide modes into sub-modes through incorporating changes of slopes or 'breaks'. The fine classification thus accommodates modes that have been subsumed by adjacent modes of greater magnitude.

Given that TM bands 1, 2, 3 and 5 are reported to be the most useful for snow mapping, as they best record the optical characteristics of snow,[6–8] they were alternately combined to produce composite images with a 2.5% linear saturation stretch in each tail. As we only had colour composites, TM bands 3-4-5 were the most suitable to our study. Boolean images of snow cover were created for each date and the area of snow cover noted. To analyse the repeated occurrence of snowfall in the study area, all 41 snow-cover maps were overlaid to create a snow-cover 'summation image'. To observe the relationship between repeated snow cover and topography, the DEM and summation image were rescaled to percentages and proportioned, which helped confirm that prolonged snow cover was favoured in the higher altitude regions. A regression of repeated snow cover against altitude was obtained and snow cover incidences determined at 50-m elevational intervals. Simple cross-tabulation change analysis techniques were also performed on the images.[9]

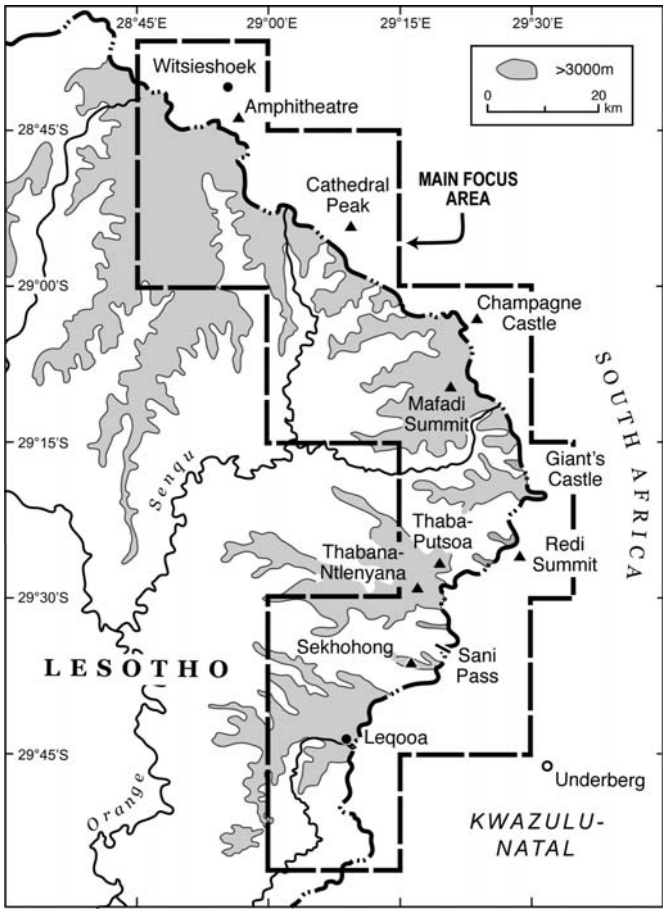

Fig. 1. Study area for which snow cover over the Drakensberg was assessed using satellite images.

Although satellite images for this study were generally available every 16 days at each satellite overpass, there were short periods when Landsat 5 TM and Landsat 7 ETM+ sensors received data concurrently, allowing for data to be captured every eight days. A further potential limitation with determining snow cover through remote sensing includes making an accurate distinction between cloud and snow from the sensor data, as the bulk optical properties of water and snow are similar in the visible and near-infrared wavelengths.[10,11] However, such problems are overcome with a sufficient database of available imagery containing cloud-free days[12] and/or through cloud detection techniques using shadow matching.[13]

Snow-cover patterns for individual months over multiple years were developed and analysed to determine monthly and seasonal trends. Images were grouped into months from May to September, but snow occurrences in April and October were not

Table 2. Synoptic precipitation-producing system types after Preston-Whyte[14] and their reclassification for snow-producing weather categories across the Drakensberg.

Synoptic type category	Potential for snow precipitation	Reclassified weather
Tropical-temperature trough	No – summer rainfall event	–
Westerly wave	Yes – where cloud extends across Drakensberg	Low pressure over the interior
(incl. cut-off low)	A cut-off low is the intense form and increases precipitation	Cut-off low
Ridging high	Yes – orographic precipitation	Onshore flow
East coast low	Infrequently – severe thunderstorms over the interior of KZN	Coastal low
High pressure	No – stable conditions	–
Easterly flow	No – rain usually confined to northern coastal KZN	–
Mid-latitude cyclone	Yes – low temperatures and brief periods of precipitation	Broad cold front
Tropical cyclone	Very seldom – the Drakensberg is too far removed	–

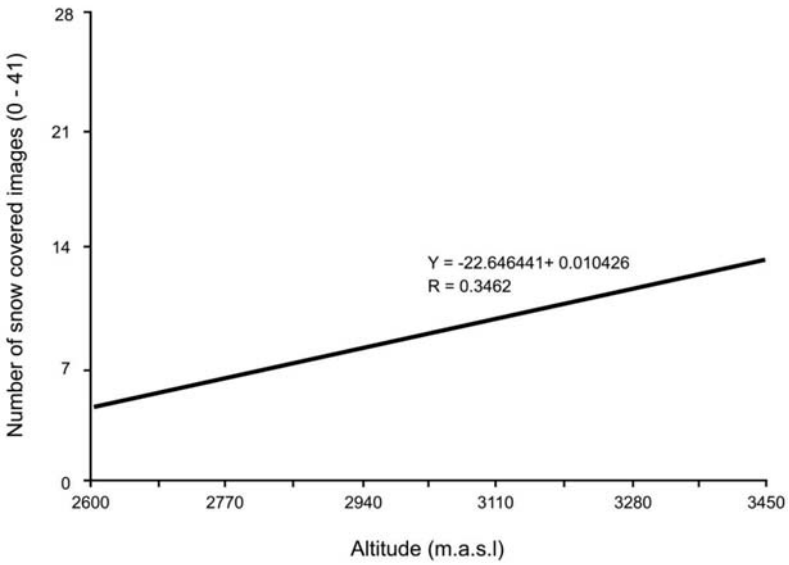

Fig. 2. Trend between altitude and the number of snow-covered images between 1989 and 2004 occurring in each pixel.

included due to low occurrences (one and three instances respectively). Images were also compiled to represent early (April–June), middle (July–August) and late (September–October) snow-season scenarios.

Daily climate data and synoptic charts were used to verify the timing of particular weather conditions responsible for snow events. Synoptic conditions conducive to producing precipitation over the Drakensberg region[14] were reclassified for snow-producing weather categories (Table 2). Underberg and Bethlehem were chosen for daily weather data as they are the closest stations to the study region that provide reliable and consistent records. The two centres are also located in different areas adjacent to the Drakensberg escarpment. Whilst Underberg is located in the foothills to the east of the southern Drakensberg, Bethlehem is situated on the plateau, north of the Drakensberg escarpment.

Results and discussion

Imagery of the repeated occurrence of snow over the study area, based on 41 images between 1989 and 2004, indicates that the maximum value for the number of incidences of the presence of snow for any pixel locality is 28 (68% occurrence), which corresponds with south-facing slopes of over 3 250 m a.s.l. A proportional relationship (R = 0.35) is recorded between the altitude of snow-covered pixels and the number of occurrences that pixels were covered in snow (Fig. 2). Snow incidences increase with altitude to about 3 250 m a.s.l., above which the median number of incidences remains constant (Fig. 3). The quartile deviation in the number of snow-cover incidences is small for lower altitudes (<3 000 m a.s.l.), while altitudes above 3 200 m a.s.l. have the highest deviation. Thus, although the frequency of snow cover increases with altitude, so does the variability. This may be attributed to lower altitudes only receiving snow during severe events when all locations along the Drakensberg become snow covered. Higher altitudes are receptive to lesser magnitude snow events, but these usually provide a more varied snow distribution across the mountain region.

The highest incidence of snow cover was recorded during the months of June to August (63% of annual total), whilst May (12%) and September (14%) had fewer recordings. Although

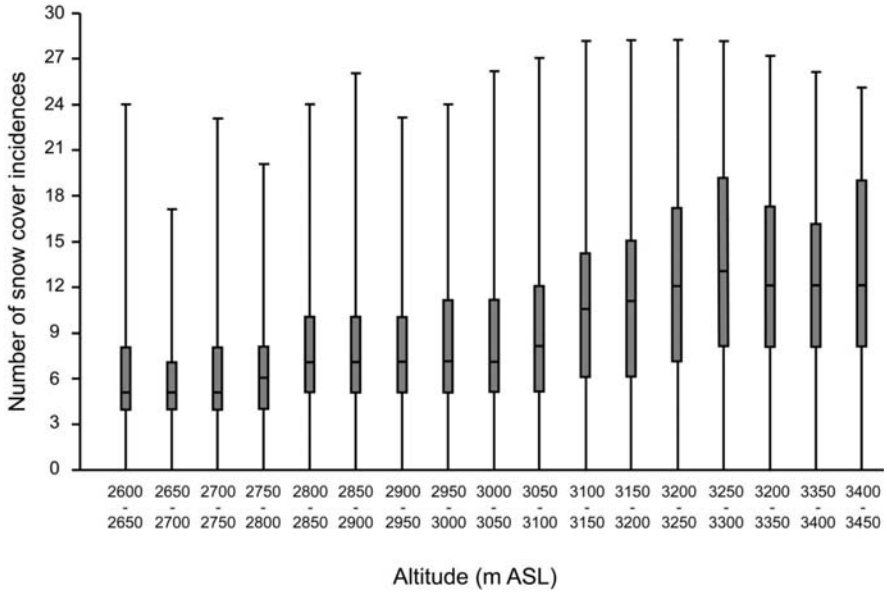

Fig. 3. Minimum, lower quartile, median, upper quartile and maximum number of incidences where a pixel was covered by snow across 41 images (1989–2004) in 50-m altitudinal classes.

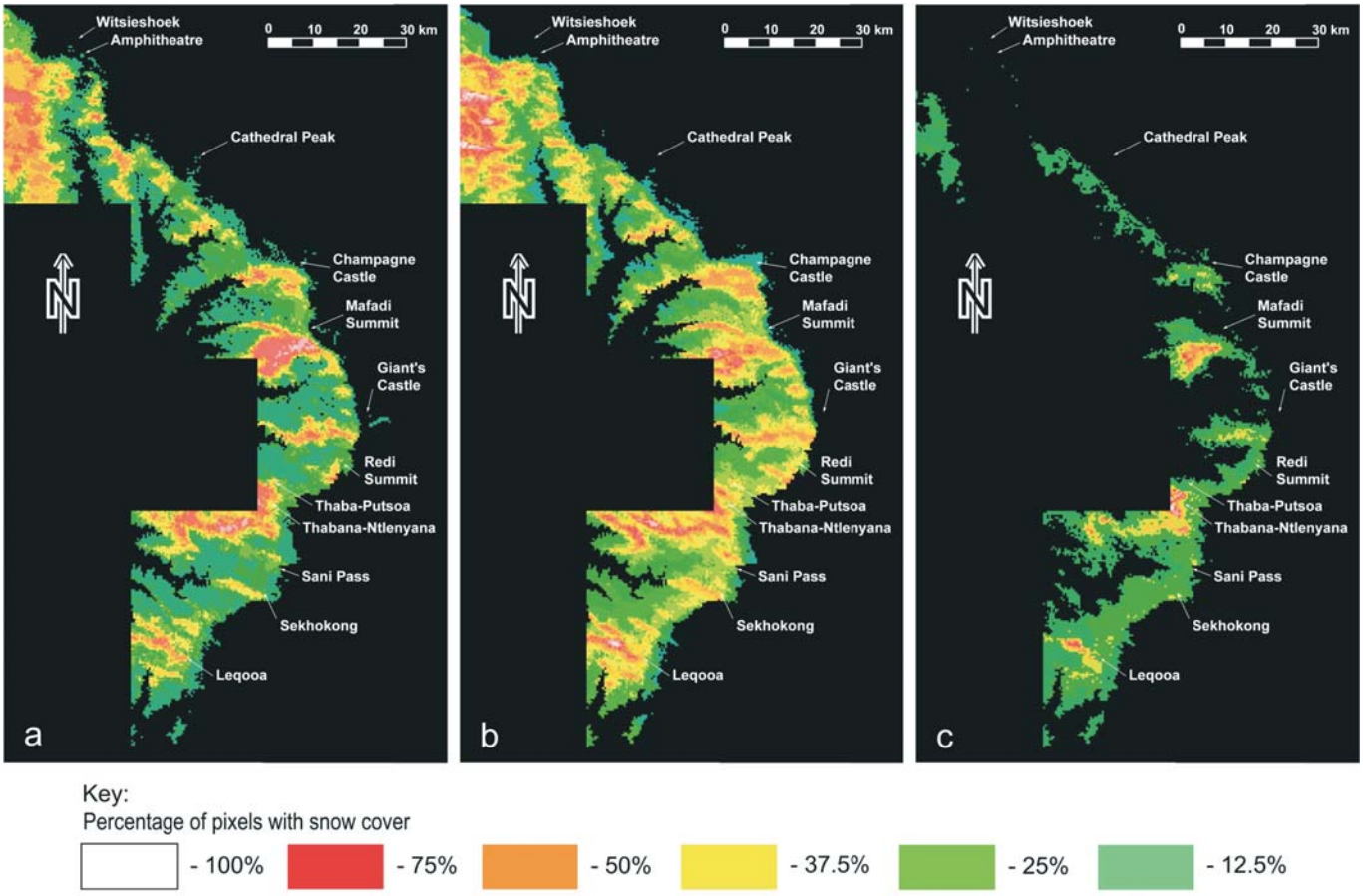

Fig. 4. Seasonal occurrence of snow over the Drakensberg from 1989 to 2004: (**a**) early snow season (April–June), (**b**) mid-snow season (July, August) and (**c**) late snow season (September, October).

snowfalls during May (autumn) were widespread across the region, they were generally restricted to altitudes over 3 000 m a.s.l. In contrast, September (spring) snowfalls occurred below 2 800 m a.s.l., but were generally confined to the central and southern Drakensberg regions. The most widespread snow cover occurred in July due to the inclusion of snow recorded at lower altitudes (2 600 m a.s.l.). Although August had the highest monthly snow incidence (29% of annual total), it was restricted to higher altitudes than the two preceding winter months due to warmer conditions. The grouping of snow-covered images into early (April–June), mid (July–August) and late (September–October) snow seasons indicated little difference in snow distribution between early and mid seasons (Fig. 4). Snow cover during the late snow season was notably less frequent north of Champagne Castle and the northwestern Lesotho highlands, which may be due to snowfall patterns and/or rapid ablation associated with warmer conditions towards the north, and thus not coinciding with the satellite overpasses.

Cold fronts (mid-latitude cyclones) account for about 66% of snowfalls over the Drakensberg and provide for a uniform spatial coverage, but extensive snow is usually restricted to altitudes above 3 000 m a.s.l (Fig. 5). Whilst strong cold front systems in mid-winter may bring extensive snow to areas below 2 600 m a.s.l., snowfalls during the passage of weaker systems are restricted to the main escarpment edge. Cut-off lows, which are usually associated with the passage of one or more cold fronts, account for about 15% of snow over the Drakensberg. Cut-off lows are responsible for the heaviest and most widespread snowfalls, and have a minimum snowfall altitude of usually below 2 600 m a.s.l. Although snow cover is uniformly high across the region, areas along the escarpment north of Giant's Castle encounter the highest incidence of snow associated with cut-off lows. Snowfall associated with low-pressure systems along South Africa's east coast are occasionally observed during late winter or early spring, and account for about 10% of snowfalls. Such snowfalls are generally restricted to altitudes above 3 000 m a.s.l. and most frequently affect the higher summits of the central Drakensberg. Low-pressure systems over the interior of the sub-continent contribute 8% of snowfalls, particularly in the northernmost Drakensberg (Witsieshoek region), but such events are mostly confined to late winter or early spring. One satellite-captured incidence of snowfall associated with 'onshore flow' was recorded during August 1990 (Fig. 5). Such snowfall was restricted to a narrow zone along the escarpment, north of Champagne Castle, and is associated with orographic uplift of relatively warm, moist Indian Ocean airflow.

Conclusion

Five types of snow-producing weather systems were identified for the Drakensberg from synoptic charts, weather data and satellite images. Cold fronts and associated cut-off lows accounted for about 80% of snow cover over the Drakensberg. The heaviest and most widespread snow occurred over the three winter months (June–August), whilst snow in spring months was frequently confined to the central and southern regions due to the contraction of the circumpolar vortex, which weakens the continental pathways of westerly waves, mid-latitude cyclones and associated cold fronts over the sub-continent.[15,16]

The spatio-temporal patterns of snow cover over the region

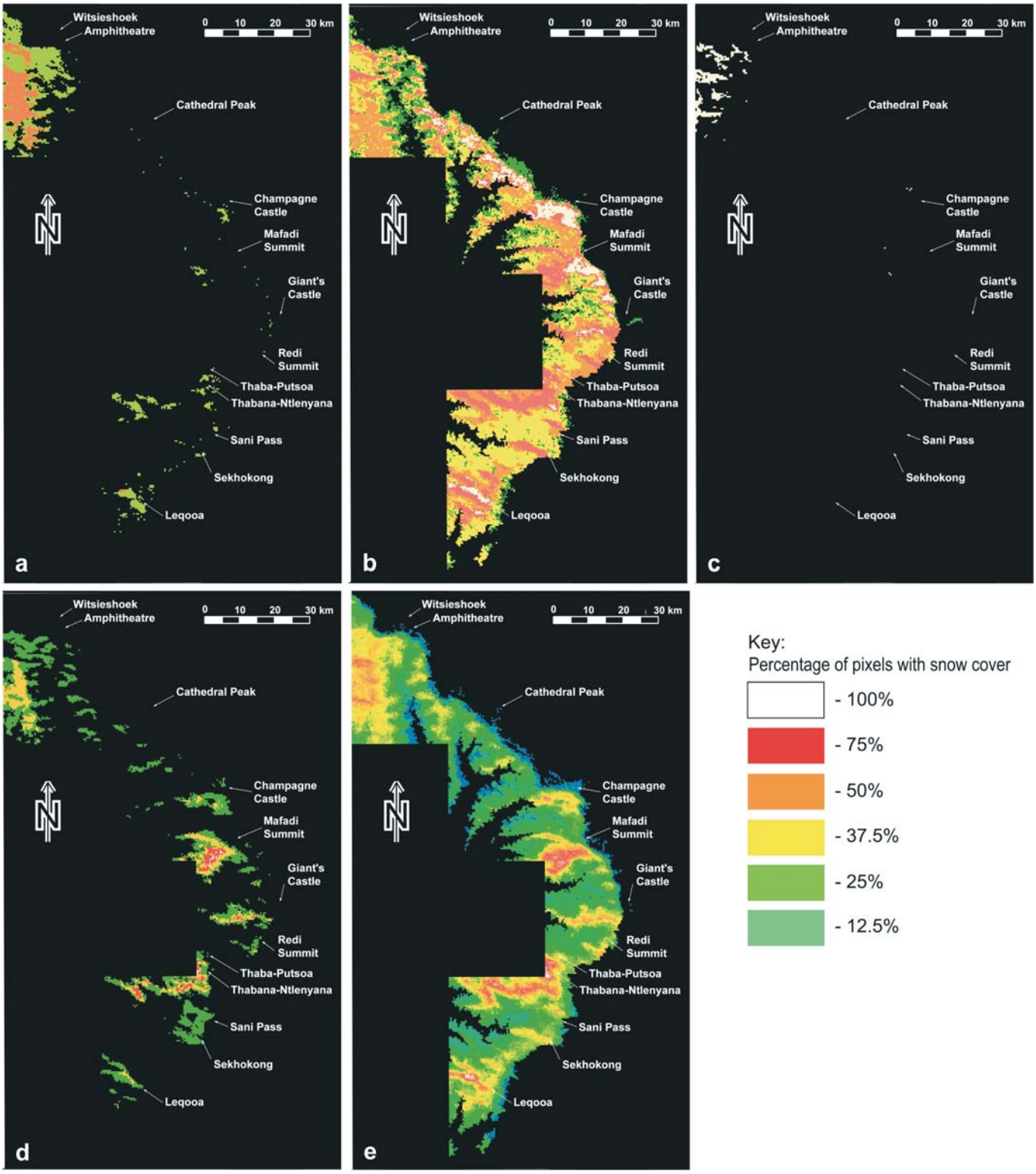

Fig. 5. Occurrence of snow cover associated with various snow-producing weather types as per Table 1: (**a**) low pressure over the interior ($n = 3$), (**b**) cut-off low ($n = 6$), (**c**) onshore flow ($n = 1$), (**d**) coastal low ($n = 4$) and (**e**) broad cold front ($n = 27$).

may impact the distribution and life cycles of fauna such as ice rats (*Otomys sloggetti*) and the timing of early flowering of certain flora across the region. In addition, an understanding of the macro-scale distribution and timing of long-term annual snow patterns may assist developers to establish infrastructures, such as roads and ski resorts, at the most suitable localities, whilst also providing important information for early warning and disaster risk reduction initiatives.

We appreciate the constructive inputs provided by two anonymous referees; these have helped improve the manuscript. This project was funded through the University of the Witwatersrand Research Incentive Scheme, for which we are thankful.

Received 4 September 2008. Accepted 18 May 2009.

1. Tyson P.D., Preston-Whyte R.A. and Schulze R.E. (1976). *The Climate of the Drakensberg*, pp. 11–76. Natal Town and Regional Planning Commission, Pietermaritzburg.

2. Schulze R.E. and McGee O.S. (1978). Climatic indices and classifications in relation to the biogeography of southern Africa. In *Biogeography and Ecology of Southern Africa,* eds M.J.A. Werger and A.C. van Bruggen, pp. 21–52. Junk, The Hague.
3. Grab S.W. (1997). Annually re-forming miniature sorted patterned ground in the high Drakensberg, southern Africa. *Earth Surf. Proc. Landforms* **22**, 733–745.
4. Mulder N. and Grab S.W. (2002). Remote sensing for snow cover analysis along the Drakensberg escarpment. *S. Afr. J. Sci.* **98**, 213–217.
5. Hall D.K., Riggs G.A. and Salomonson V.V. (1995). Development of methods for mapping global snow cover using Moderate Resolution Image Spectroradiometer (MODIS) data. *Remote Sens. Env.* **54**, 137–140.
6. Dozier J. (1989). Spectral signature of alpine snow-cover from Landsat Thematic Mapper. *Remote Sens. Env.* **28**, 9–22.
7. Hall D.K., Chang A.T.C. and Foster J.L. (1999). *BOREAS RSS-08 snow maps derived from Landsat TM imagery.* ORML Distributed Active Archive Centre, Oak Ridge National Laboratory, Oak Ridge, Tennessee. Online from: http://eosdis.ornl.gov
8. Derksen C. and LeDrew E. (2000). Variability and change in terrestrial snow cover: data acquisition and links to the atmosphere. *Prog. Phys. Geog.* **24**, 469–498.
9. Singh A. (1989). Digital change detection techniques using remotely-sensed data. *Int. J. Remote Sens.* **10**, 989–1003.
10. Dozier J. (1991). *Remote sensing of alpine snow cover: invisible and near-infrared wavelengths.* Proceedings from the Centre for Snow Science at Alta 1991 Symposium: Online at: http://www.avalanche.org/~moonstone/cssa91′.htm
11. Rosenthal W. and Dozier J. (1996). Automated mapping of montane snow cover at subpixel resolution from the Landsat Thematic Mapper. *Water Resour. Res.* **32**, 115–130.
12. Peterson J.A., Chandra S. and Lundberg C. (2004). Landforms from the Quaternary glaciations of Papua New Guinea: an overview of ice extent during the Late Glacial Maximum. In *Quaternary Glaciations – Extent and Chronology, Part III: South America, Asia, Africa, Australia, Antarctica,* eds J. Ehlers and P.L. Gibbard, pp. 313–336. Elsevier, Amsterdam.
13. Choi H. and Bindschadler R. (2004). Cloud detection in Landsat imagery of ice sheets using shadow matching technique and automatic normalized difference snow index threshold value decision. *Remote Sens. Env.* **91**, 237–242.
14. Preston-Whyte R.A., Diab R.D. and Washington R. (1991). Diurnal variation of rainfall events by synoptic type in Natal. *S. Afr. Geogr. J.* **73**, 22–28.
15. Budin G.R. (1985). Interannual variability of Australian snowfall. *Aust. Met. Mag.* **33**, 145–159.
16. Preston-Whyte R.A. and Tyson P.D. (1997). *The Atmosphere and Weather of Southern Africa.* Oxford University Press, Cape Town.